

Detecting Juno’s ‘Heartbeat’: Communications Support during Critical Events of the Juno Mission

Dustin Buccino
(818) 393 – 1072

Dustin.R.Buccino@jpl.nasa.gov

Melissa Soriano
(818) 393 – 7632

Melissa.A.Soriano@jpl.nasa.gov

Kamal Oudrhiri
(818) 393 – 1143

Kamal.Oudrhiri@jpl.nasa.gov

Susan Finley
(818) 354 – 5669

Susan.G.Finley@jpl.nasa.gov

Daniel Kahan
(818) 393 – 2803

Daniel.S.Kahan@jpl.nasa.gov

Oscar Yang
(818) 354 – 5747

Oscar.Yang@jpl.nasa.gov

Andre Jongeling
(818) 393 – 2404

Andre.P.Jongeling@jpl.nasa.gov

Jet Propulsion Laboratory, California Institute of Technology
4800 Oak Grove Dr.
Pasadena, CA 91109

Abstract—Since launch, radio science has been a key component of the Juno mission to Jupiter. The prime objective of the radio science investigation is to estimate the gravitational field of Jupiter from the Doppler shift on the radio link between the spacecraft and the Earth-based observing antennas of NASA’s Deep Space Network (DSN). In addition to estimation of the gravitational field, radio science has provided critical engineering support to the Juno mission. Utilizing high-sensitivity open-loop receivers and real-time signal processing, radio science is able to detect the ‘heartbeat’ of the Juno spacecraft and determine the current state of the spacecraft. The Juno spacecraft utilizes two frequencies for communication with Earth: the telecommunications system X-band link and the radio science Ka-band link. Radio science has provided communications monitoring support for the spacecraft launch in 2011, spacecraft main engine firings (including Deep Space Maneuvers in 2012 and Jupiter Orbit Insertion in 2016), the Earth gravity assist flyby in 2013, and times when the spacecraft was off-Earth point during Jupiter closest approach with a weak signal level. By measuring the signal-to-noise ratio, received carrier frequency, and subcarrier frequency of the X-band downlink signal in real-time, radio science is able to determine the state of the spacecraft in scenarios where the link margin is not sufficient to support telemetry. An off-nominal spacecraft state will change the signal-to-noise level, subcarrier frequency, and spin modulation of the carrier frequency which are detectable in the open-loop receiver of the DSN. With the addition of multiple frequency shift keying (MFSK) ‘tones’ encoding, the subcarrier frequency can be changed onboard the spacecraft for determination of selected events by the flight team. Tones were utilized during main engine firings on Juno, including Jupiter Orbit Insertion (JOI). Tones are decoded in near real-time by the Entry, Descent, and Landing (EDL) Data Analysis (EDA) system downstream of the DSN open-loop receivers. Robust implementation of hardware, software, and operations planning has ensured successful data collection and real-time status reporting of spacecraft state to the Juno mission. Lessons learned from communicating with Juno in this way while in the harsh environment of Jupiter are documented and discussed in the context of upcoming missions to Jupiter.

TABLE OF CONTENTS

| | |
|--|----|
| 1. INTRODUCTION | 1 |
| 2. SYSTEM OVERVIEW | 2 |
| 3. SIGNAL ANALYSIS | 4 |
| 4. LAUNCH | 8 |
| 5. DEEP SPACE MANEUVERS | 8 |
| 6. EARTH FLYBY | 10 |
| 7. JUPITER ORBIT INSERTION (JOI) | 11 |
| 8. PERIJOVES | 14 |
| 9. CONCLUSION | 15 |
| ACKNOWLEDGEMENTS | 16 |
| REFERENCES | 16 |
| BIOGRAPHY | 17 |

1. INTRODUCTION

Juno is a National Aeronautics and Space Administration (NASA) New Frontiers mission to Jupiter. The solar-powered Juno spacecraft was launched on August 5, 2011. Set on a five-year interplanetary cruise, Juno performed a series of two Deep Space Maneuvers (DSMs) on August 30, 2012, and September 14, 2012, followed by an Earth flyby on October 9, 2013. Juno arrived at Jupiter on July 5, 2016, and entered into a 53-day orbit around the planet. Juno is in a highly-elliptical, polar orbit with an altitude of closest approach (perijove) of 3500 km above the 1-bar level surface. Juno is a two rotation-per-minute (2 RPM) spin-stabilized spacecraft. An originally-planned maneuver to enter into a 14-day orbit was cancelled due to an issue with the propulsion system. Juno is investigating the interior of the planet by measuring the gravitational and magnetic fields; investigating the atmosphere with a microwave radiometer, a visual camera and an infrared camera; and investigating the magnetosphere with high-energy particle detectors, a magnetometer, and ultraviolet spectrometer [1].

Radio science utilizes the telecommunications link between the spacecraft and the Earth-observing antennas of NASA’s

Deep Space Network (DSN) to measure atmospheric properties, orbital motion, gravitational field, and surface properties of a celestial body [2]. On Juno, the primary goal of the radio science investigation is to utilize Juno’s X-band radio transponder and Ka-band radio translator to determine the planet’s gravitational field parameters. Improved knowledge of the gravitational field of Jupiter will constrain models of the interior structure [3][4]. In addition to the primary goal of providing science support, the Juno Radio Science Team also provides engineering support to the Juno mission during critical spacecraft events. The same open-loop receiver equipment at the DSN utilized for high-precision, low-noise measurements of the radio signal provides valuable insight into the received signal-to-noise level, carrier frequency, and subcarrier frequency ‘heartbeat’ sent from the spacecraft. During critical events, where the signal power level and carrier frequency are unable to be locked by the phase-lock loop of the closed-loop receivers, the open-loop receivers can still detect and decode information from the spacecraft. During critical events, the Juno spacecraft sends an X-band signal in a carrier-only or carrier and subcarrier configuration (i.e., no ranging or telemetry signals modulated onto the carrier) from an antenna onboard the spacecraft to the ground stations of the DSN.

During main engine maneuvers, the spacecraft encodes multiple frequency shift keying (MFSK) ‘tones’ by modulating a varying-frequency subcarrier onto the carrier. The frequency of this subcarrier corresponds with a particular spacecraft event or state and is used to determine spacecraft health and diagnosis of any anomalies. The subcarrier frequency is decoded in real-time by the Entry, Descent, and Landing Data Analysis (EDA) systems [5]. This method of communication was also used on the Mars Science Laboratory rover mission [6][7].

From launch in 2011, there have been numerous critical events supported by the Juno Radio Science Team: launch, the main engine firings Deep Space Maneuver (DSM) 1 and 2, the Earth gravity assist flyby, the main engine firing during Jupiter Orbit Insertion (JOI), and perijoves with multiple challenging configurations and geometries. Table 1 shows a summary of each event.

The first section of this paper summarizes the radio systems of the spacecraft, the antennas of the DSN, and signal processing performed in real-time on the ground to support the critical activities. The second section goes into detail on each of the critical events with details of the radio science support and results of each event. Finally, the paper is concluded with a discussion of future planned supports and capabilities of radio science support during critical events.

2. SYSTEM OVERVIEW

The Juno radio science system utilizes the spacecraft telecommunications system onboard the Juno spacecraft and the Earth-based observing stations of the Deep Space Network. Juno’s telecommunication system is composed of

Table 1. Critical events of the Juno mission to Jupiter.

| Event | Date (UTC) | Description |
|-------------------------|---|--|
| Launch | Aug 5, 2011 | Spacecraft launch on the Atlas V rocket, separation and solar array deployment |
| Deep Space Maneuver 1 | Aug 30, 2012 | First main engine firing, spacecraft on a low gain antenna |
| Deep Space Maneuver 2 | Sept 14, 2012 | Main engine firing, spacecraft on a low gain antenna |
| Earth Flyby | Oct 9, 2013 | Flyby of Earth as a gravity assist en-route to Jupiter |
| Jupiter Orbit Insertion | July 5, 2016 | Large main engine firing to enter orbit around Jupiter within the high radiation and dynamic environment |
| Perijoves | Occurring every 53 days since August 27, 2016 | Periods of closest approach, diving into the radiation to get science measurements |

an X-band (8.4 GHz) communications link and a Ka-band (32 GHz) radio science link. A generalized diagram is shown in Figure 1, showing the systems which are described in detail in the following sections.

Spacecraft Telecommunications Subsystem

The Juno spacecraft has three onboard transponders. Two redundant JPL-designed Small Deep Space Transponders (SDST) provide the X-band communications support, and an Italian-designed Ka-band Translator (KaT) provides Ka-band radio science support. The KaT was designed and built by Thales Alenia Space-Italy and provided to the Juno project by the Italian Space Agency (ASI). The SDST receives and decodes uplink commands transmitted from the DSN at 7.1 GHz and encodes downlink data packets for transmission to the ground at 8.4 GHz, amplified with a Traveling Wave Tube Amplifier (TWTA). The KaT receives an uplink carrier signal from the DSN at 34 GHz and retransmits that carrier back to the ground at 32 GHz, amplified with a Solid State Power Amplifier (Ka-SSPA) [8].

The spacecraft has a High Gain Antenna (HGA) and a Medium Gain Antenna (MGA) co-pointed in the spacecraft spin direction. Additionally, there are a set of three Low Gain

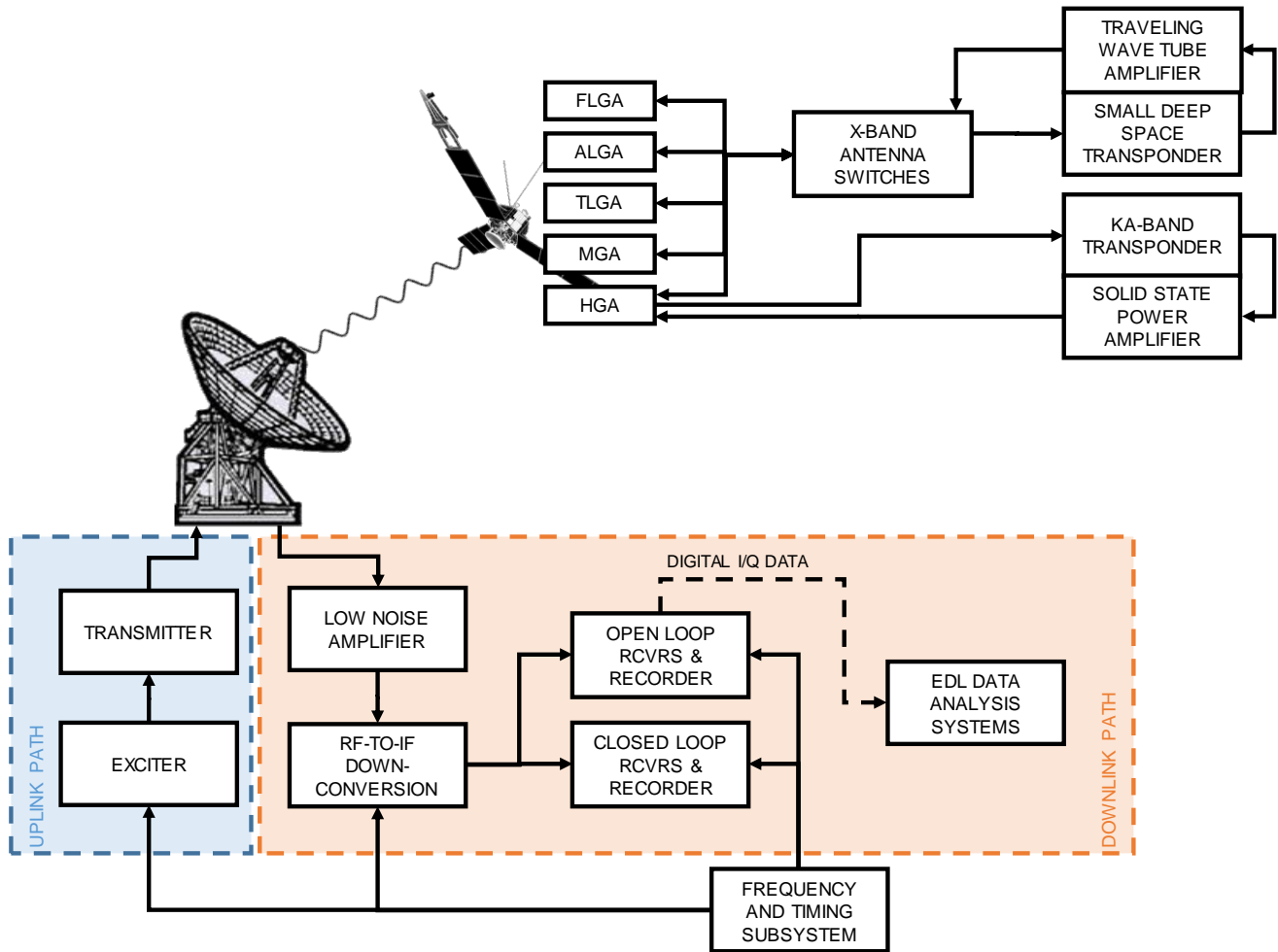


Figure 1. Generalized diagram of radio communications between a Deep Space Network antenna (bottom left) and the Juno spacecraft (top right).

Antennas (LGAs) spaced around the spacecraft in the forward direction (FLGA), aft direction (ALGA), and along the spin plane in a toroidal pattern (TLGA). All antennas are capable of X-band communications, but only the HGA is capable of Ka-band communications [9].

When the spacecraft is receiving an uplink signal from the DSN, the transponders lock onto the received uplink carrier frequency and retransmits it back to Earth phase-coherently. This is known as a *coherent* configuration. When no uplink signal is present, the transponders uses an auxiliary oscillator for frequency reference. This is known as a *non-coherent* configuration.

Deep Space Network Ground Stations

The DSN is a set of large-aperture antennas grouped into three complexes across the globe in Goldstone, California, Madrid, Spain, and Canberra, Australia. Each complex contains a set of 34-meter antennas and one 70-meter large-aperture antenna. The complexes are spaced approximately 120 degrees apart in longitude for continuous communications with a spacecraft as the Earth rotates. Each DSN antenna provides uplink and downlink support.

In a typical coherent communications or radio science pass, an uplink signal is generated by the complex's hydrogen maser Frequency and Timing System (FTS). The signal is upconverted to the correct frequency and encoded with data with an uplink exciter. The signal is then amplified by a transmitter system and sent out the horn through the antenna. This is considered the *uplink path*, and one uplink path exists for each band [10]. Special upgrades were made to the DSS-25 antenna in Goldstone, CA, to support Ka-band uplink for the Juno radio science investigation, including the installation of a Ka-band transmitter [3].

With or without the uplink path, a similar *downlink path* operates at each band. The signal is received at the antenna and amplified through a Low Noise Amplifier (LNA). The incoming analog signal is down-converted to an Intermediate Frequency (IF) with a center frequency of 300 MHz. The IF signal is distributed among the various receivers [10].

Closed-loop receivers utilize a Phase-Locked Loop (PLL) to lock on and track the spacecraft's signal. The closed-loop receiver performs subcarrier and symbol tracking to decode and provide spacecraft tracking, ranging, engineering, and science telemetry to the mission.

Open-loop receivers by nature do not actively track the carrier, but rather utilize a prediction of the frequency to sample the full spectrum around the spacecraft’s center frequency (carrier frequency). A local oscillator within the open-loop receivers down-converts the IF signal to a local frequency that is specified by the user’s predicted frequency (called the “predict”). Typically, the predict is the best-guess of the spacecraft’s received frequency, taking into account the Doppler shift on the radio link, and the spacecraft’s signal is then aligned as close to baseband as possible. This local frequency is digitized into In-phase and Quadrature (IQ) samples for recording. Open-loop recordings provide much greater flexibility for signal processing. Firstly, they have the ability to track spacecraft during high-dynamic or low-signal level events where the closed-loop receiver would not be able to track with a PLL—for example, during Entry, Descent, and Landing [6]. Secondly, they allow for reprocessing of the signal for higher precision radio science measurements. There are three types of open-loop receivers used during the Juno era, but each of them function in a similar capacity and are generically referred to as “open-loop receivers.” The Radio Science Receiver (RSR) is an older system designed primarily for Radio Science investigations. The Wideband Very-Long Baseline Interferometry (VLBI) Science Receiver (WVSR) was designed primarily for VLBI and radio astronomy investigations. In 2019, both the RSR and WVSR were replaced by the Open-Loop Receiver (OLR).

EDL Data Analysis Systems

The Entry, Descent, and Landing (EDL) Data Analysis (EDA) systems take in a data stream from the open-loop receivers in near real time and process the IQ samples using Fast Fourier Transform (FFT) based algorithms to acquire and track the signal. The EDA tracks the main carrier and subcarrier frequencies to decode the Multiple Frequency Shift Keying (MFSK) “tones” embedded in the signal. As the spacecraft undergoes a given event, the onboard flight software commands a different subcarrier frequency. Thus, the difference between the carrier and subcarrier frequencies

corresponds to an event that has taken place onboard the spacecraft, and the EDA detects the subcarrier frequency, thus the event. Each EDA is a high-power computer server with multiple threads and provides displays to the operators and the mission operations team on the messages conveyed by the tones, as well as plots of carrier and subcarrier frequency and power.

3. SIGNAL ANALYSIS

Signal Characteristics and Detection Probability

A subcarrier-encoded signal $s(t)$ received at the DSN for recording and processing can be described as [7]:

$$s(t) = \sqrt{2P_t} \cos \left[2\pi \int_{-\infty}^t d\tau \cdot f_c(\tau) + \Delta \cdot Sqr \left(2\pi \int_{-\infty}^t d\tau \cdot f_d(\tau) \right) \right] + n(t) \quad (1)$$

where f_c is the carrier frequency, f_d is the subcarrier frequency, Δ is the modulation index (a measure of how much power is split between the carrier and subcarrier), P_t is the total power, and $n(t)$ is the noise component. The function $Sqr(x)$ is the hard-limited sine function:

$$Sqr(x) = \begin{cases} 1 & 0 < x \leq \pi \\ -1 & \pi < x < 2\pi \end{cases} \quad (2)$$

The down-converted signal, as recorded on the open-loop receiver, is Doppler-compensated (Section 2). The residual frequency is defined as:

$$\delta f = f_c - f_p \quad (3)$$

where δf is the residual frequency and f_p is the predicted frequency. The observables from this signal are described in Table 2.

Table 2. Observables from the received signal.

| Symbol | Observable | Description and Information Contained |
|---------------|---|---|
| f_c | Carrier Frequency | Total Doppler-shifted frequency of the downlink signal. |
| f_d | Subcarrier Frequency | Offset of the subcarrier from the carrier. The subcarrier can be modulated to embed telemetry, or the subcarrier frequency can be changed onboard to convey basic information called tones. |
| δf | Residual Frequency | Deviations from the nominal expected signal. Indicative of dynamical effects experienced by the spacecraft. |
| P_c | Carrier Power ($P_c = P_t \cos^2 \Delta$) | Power in the main carrier. Differences from the expected level can indicate propagation effects (e.g. atmospheric absorption) or spacecraft off-axis pointing. |
| P_c/No | Carrier Power to Noise Ratio | |
| P_d | Data Power ($P_d = P_t \sin^2 \Delta$) | Should be proportional to the total carrier power by the modulation index Δ |
| P_d/No | Data Power to Noise Ratio | |
| P_{tone} | Tone Power ($P_{tone} = P_d/1.2337$) | Should be proportional to the data power. |
| P_{tone}/No | Tone Power to Noise Ratio | |

The open-loop receivers record the IQ values on the down-converted signal $s(t)$. A sampling rate (f_s) is selected such that the entire spectrum can be recorded, with extra bandwidth to compensate for unknown dynamical effects. For Juno, 100-kHz recordings at 8-bit resolution are sufficient to capture the carrier and subcarrier during critical events. 50-kHz recordings at 8-bit resolution were sufficient for Jupiter Orbit Insertion, due to the limited range of subcarrier frequencies.

An initial Fast Fourier Transform (FFT) is performed on the open-loop receiver. The FFT takes a given number of IQ values (N_{FFT}), zero-fills by a multiplicative factor (zf) for higher-precision frequency interpolation, and repeats for a number of cycles to average together multiple FFTs (N_A). The number of averages and number of points must be balanced to detect the signal but not smear any dynamical effects. The total incoherent integration time T is calculated as:

$$T = \frac{N_A \cdot N_{FFT}}{f_s} \quad (4)$$

with corresponding frequency resolution Δf (also called the bin size):

$$\Delta f = \frac{f_s}{N_{FFT} \cdot zf} \quad (5)$$

The EDAs utilize a series of FFT algorithms to detect the frequency of the subcarrier (f_d), divided into an acquisition state and a tracking state. During the acquisition state, the EDA searches a larger frequency space (the sampling rate, f_s) for the carrier signal using an FFT, similar to that of the open-loop receiver. In addition to a standard FFT, the EDA also searches across a range of frequency rates (\dot{f}) at step size ($\Delta \dot{f}$). This gives the search space two dimensions: frequency

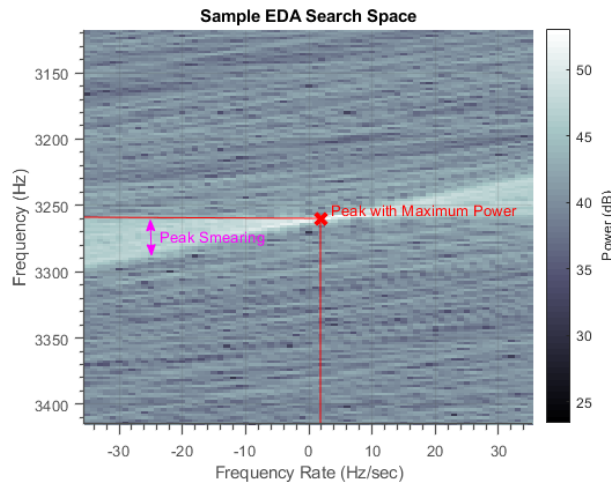


Figure 2. A sample search space from the EDA, which has been zoomed in to the area of interest. The peak is marked with a red X. Areas not near the peak are smeared due to the dynamics of the signal.

and frequency rate, as shown in Figure 2. The EDA must search across these two dimensions. Even though the signal recorded by the open-loop receiver attempts to compensate for all known Doppler effects, there are residual dynamical effects which smear the signal across multiple frequency bins. This smearing effect reduces the signal-to-noise ratio and thus the probability of detection. The tracking state reduces the search space by forward predicting the most probable frequency of the carrier based on the previous frequency and frequency rate, allowing for a more refined estimate of carrier and subcarrier frequency.

The probability of detecting any given carrier frequency or subcarrier frequency correctly is defined with a probability density function, derived based on the assumption of a chi-squared distribution of the signal in the frequency bins [7][11]. The probability of detecting the carrier is given as:

$$P = \int_{x=0}^{x=+\infty} I_{m-1}(\sqrt{4 \cdot x \cdot T \cdot Pc/No}) e^{-(x+T \cdot Pc/No)} \left(\frac{x}{T \cdot Pc/No} \right)^{\frac{M-1}{2}} \left[1 - \frac{\Gamma(M, x)}{\Gamma(M)} \right]^{N_f-1} dx \quad (6)$$

where T is the incoherent integration time, Pc/No is the carrier signal-to-noise ratio, M is the product of the frequency resolution and integration time ($M = T\Delta f$), and N_f is the total number of FFT bins to search over. The Euler gamma function and incomplete gamma function are $\Gamma(M)$ and $\Gamma(M, x)$, respectively. Assuming the carrier was detected correctly, the probability of correct tone detection (subcarrier frequency) is:

$$P = \int_{x=0}^{x=+\infty} I_{m-1}(\sqrt{4 \cdot x \cdot T \cdot P_{tone}/No}) e^{-(x+T \cdot P_{tone}/No)} \left(\frac{x}{T \cdot P_{tone}/No} \right)^{\frac{M-1}{2}} \left[1 - \frac{\Gamma(M, x)}{\Gamma(M)} \right]^{N_t-1} dx \quad (7)$$

The key difference between Eq. (6) and Eq. (7) is the number of bins has been replaced by the number of tones N_t , the signal-to-noise ratio has been replaced by the tone power-to-noise ratio P_{tone}/No , and the product M is now twice the previous ($M = 2T\Delta f$).

The driving factors in both Eq. (6) and Eq. (7) are the incoherent integration time T , frequency resolution Δf , the number of search items (N_f or N_t), and the respective signal-to-noise ratios (Pc/No or P_{tone}/No). This is the primary trade space for event detection with tones.

System Configuration

For a 50-kHz sampling rate, 3-10 second incoherent integration time is desired on the open-loop receivers as a balance between time resolution and the signal-to-noise ratio. This interval was selected based upon the anticipated Doppler

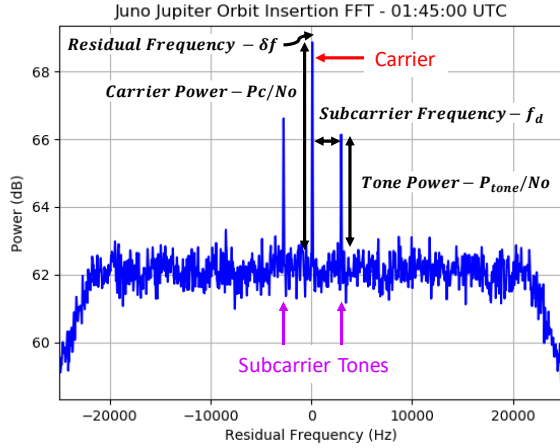


Figure 3. FFT of a signal from Juno with a carrier signal and subcarrier "tone". The observables from Table 2 are marked.

dynamics and P_c/No . The typical setting is $N_{FFT} = 1024$, $z_f = 4$, $N_A = 150$ for ~ 3 second integration time. An example of this is shown in Figure 3, with each of the observables annotated.

For the DSM and JOI maneuvers, MFSK tones are used. The IQ values recorded by the open-loop receiver are encoded into a binary bit stream and sent across the JPL flight operations network from the receiver at the DSN complex to the EDAs for tone detection. The EDAs are located at two Mission Support Areas: the Jet Propulsion Laboratory (Pasadena, CA) and Lockheed Martin Space Systems (Littleton, CO).

The EDAs are configured with FFT settings as an optimization between the expected spacecraft dynamics and the expected signal-to-noise ratio of the signal. Tones were used during the Deep Space Maneuvers in 2012 and Jupiter Orbit Insertion in 2016, both main engine maneuvers critical for the success of the mission. The dominating dynamics experienced by the spacecraft, and the downlink signal, were:

- Dynamics from the spacecraft trajectory flight path, including velocity change from main engine firing
- Spacecraft attitude adjustments to/from maneuver attitude
- Doppler spin signature caused by the TLGA being offset from the spin axis of the spacecraft (2-5 RPM)

The EDA configuration parameters are selected based on the expected Doppler frequency dynamics provided by the Juno navigation team. The navigation team computes the expected uncertainties in the line-of-sight velocity and acceleration of the spacecraft, which are then converted into an expected Doppler frequency residual. The maximum frequency residual (f_{max}), residual frequency rate (\dot{f}_{max}), and residual frequency acceleration (\ddot{f}_{max}) drive the configuration. The

general rules of thumb [12] assume a well-behaved frequency acceleration ($\ddot{f} \approx 0$ Hz/s/s):

$$\Delta f > \sqrt{4\dot{f}_{max}} \quad (8)$$

$$T < \sqrt{2\frac{\Delta f}{\ddot{f}_{max}}} \quad (9)$$

Dynamics from the spacecraft trajectory flight path are largely predictable. The open-loop receivers provide an initial Doppler compensation to remove the effects, but any trajectory prediction has a level of uncertainty associated with it. Because of the unique arrival geometry of Juno at Jupiter, a minimal amount of the spacecraft's velocity is projected onto the line-of-sight, which minimizes the Doppler shift on the signal [4]. The Juno navigation team estimated uncertainties in the trajectory during JOI of a maximum of ~ 90 Hz (Figure 4). Because the uncertainty changes slowly over time, the maximum frequency rate and frequency acceleration from the uncertainty in trajectory are small at 0.05 Hz/s and 0.0005 Hz/s/s, respectively. During

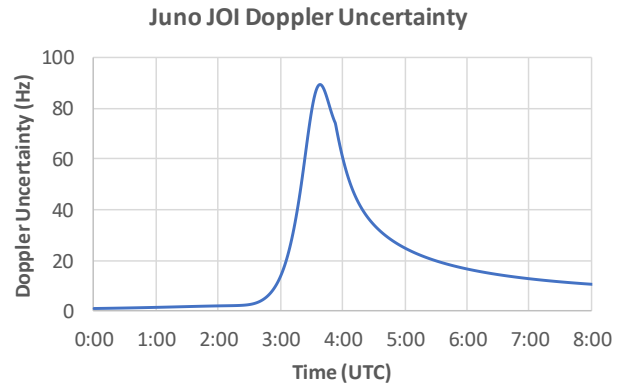


Figure 4. Doppler uncertainty derived from the uncertainty in the spacecraft trajectory during JOI

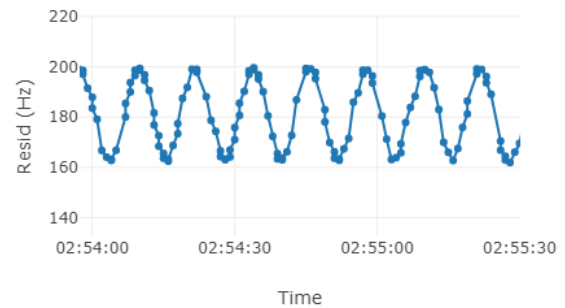


Figure 5. Spin signature from the Toroidal Low Gain Antenna, which has an amplitude of 17.5 Hz and period of 12 seconds.

main engine maneuvers, the spacecraft is spin-stabilized at 5 RPM, instead of the usual 2 RPM during normal operations. The TLGA, the primary antenna utilized during main engine maneuvers, is offset from the spin axis [9], which induces a Doppler spin signature caused by the relative motion of the antenna with respect to the spin axis. The spin signature is sinusoidal in nature with an amplitude of 17.5 Hz and periodicity of 12 seconds (Figure 5). The maximum frequency rate and acceleration from the spin signature are ~ 9.2 Hz/sec and ~ 4.8 Hz/s/s, respectively.

Table 3 shows a summary of the input parameters to estimate the tones performance during the DSM and JOI main engine maneuvers. Using these inputs to Eq. (8) and Eq. (9), the FFT resolution Δf should be 5 Hz and integration time T should be 2 seconds (rounding to integer values, required by the software), which help derive the rest of the main EDA signal processing parameters shown in Table 4.

The probability of correct detection of the tones is computed with Eq. (6) and Eq. (7). However, the assumptions in the theoretical model and the “rules of thumb” assume a well-behaved frequency acceleration (i.e. $\dot{f} \approx 0$ Hz/s/s). The spin signature introduces a clear frequency acceleration. In order to account for the frequency accelerations, simulations were performed. An artificial digital signal with MFSK tones encoded and the expected Doppler dynamics from the spin signature was generated at various signal-to-noise ratios and run through the EDA with the Juno configuration. The total number of recovered tones from the EDA in the Juno configuration was compared against the generated signal. Tone errors were then computed for each signal-to-noise ratio. The simulations show that, to recover 99.9% of tones, an additional 1-1.5 dB-Hz is required over the theoretical prediction.

The probability of error (inverse of correct tone detection) is shown in Figure 6. Theoretical probability of error is shown in blue, with no acceleration assumed. Simulated data with

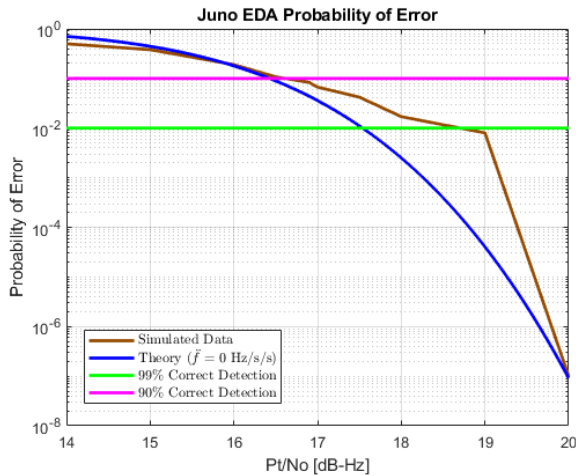


Figure 6. Probability of error for Juno's dynamics and EDA configuration. Simulations deviate from the theory due to the large frequency accelerations from the spin signature.

Table 3. Key input parameters for Juno EDA configuration and performance evaluation.

| Parameter | Value |
|--|-----------------|
| Tone Configuration | |
| Modulation Index (Δ) | 48 |
| Number of Tones (N_t) | 512 |
| Initial Tone Frequency | 2000.927925 Hz |
| Final Tone Frequency | 22875.951349 Hz |
| Tone Frequency Delta | 40.769577 Hz |
| Link Budget | |
| DSM-1 – Pt/No (DSS-14) | 20.4-22.9 dB-Hz |
| DSM-2 – Pt/No (DSS-14) | 21.2-22.9 dB-Hz |
| JOI – Pt/No (DSS-14) | 15.1-19.3 dB-Hz |
| Frequency Dynamics | |
| Max Frequency Rate (\dot{f}_{max}) | <10 Hz/s |
| Max Frequency Accel (\ddot{f}_{max}) | <5 Hz/s/s |

Table 4. Key EDA configuration parameters for Juno.

| Parameter | Acquisition State Value | Tracking State Value |
|---|-------------------------|----------------------|
| FFT Resolution (Δf) | 5.0 Hz | 5.0 Hz |
| Number of Samples (N_{FFT}) | 10000 | 10000 |
| Coherent Integration Time (τ) | 0.2 sec | 0.2 sec |
| Incoherent Integration Time (T) | 3.0 sec | 3.0 sec |
| Number of Averaged FFTs (M) | 15 | 15 |
| Carrier Frequency Search Range | ± 1000 Hz | ± 50 Hz |
| Subcarrier Frequency Search Range | ± 10 Hz | ± 2 Hz |
| Pre-FFT Frequency Rate Search (\dot{f}_{pre}) | ± 15 Hz/s | ± 15 Hz/s |
| Pre-FFT Frequency Rate Bins ($N_{r,pre}$) | 7 | 7 |
| Post-FFT Frequency Rate Search (\dot{f}_{post}) | ± 10 Hz/s | ± 10 Hz/s |
| Post-FFT Frequency Rate Bins ($N_{r,post}$) | 9 | 9 |
| Threshold SNR | 10.0 dB-Hz | 10.0 dB-Hz |
| Tracking Loop Feedback State | off | off |
| Total Search Space (N_f) | 150,000 | 150,000 |

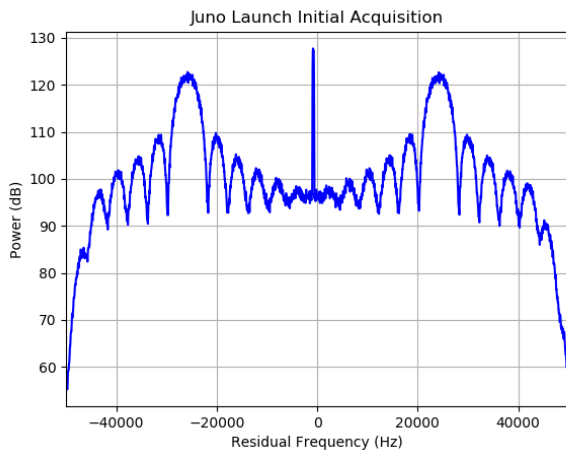


Figure 7. The full spectrum of Juno’s signal right after initial acquisition. The carrier peak is seen in the middle, and the telemetry-encoded subcarriers are seen on either side at ± 25 kHz.

the expected Juno spin dynamics was generated and processed to obtain the probability of error shown in brown. The requirement of 99% correct detection can be met for DSM-1 and DSM-2 with a single 70-meter station (DSS-14 or DSS-43), but for JOI, it cannot be met with a single station. The solution is to increase signal-to-noise ratio by arraying together multiple antennas using the DSCC Downlink Array (DDA).

4. LAUNCH

Juno was launched on August 5, 2011, from Cape Canaveral Air Force Base on an Atlas V rocket. The Juno Radio Science team was supporting the launch for initial acquisition of the spacecraft by the DSN. The primary purpose for radio science support was a contingency scenario if the closed-loop receivers could not lock to the signal at the expected time. In this case, the Radio Science team would begin a wide-band frequency search with the open-loop receivers for Juno’s downlink signal.

Launch was a success with liftoff occurring at 16:25:00 UTC, though no signal would be expected until after separation from the launch vehicle. Separation occurred approximately 53 minutes later at 17:18:06 UTC. The spacecraft powered on the SDST and the X-band TWTAs transitioned to high power mode to enable communications 11 seconds after separation (17:18:17 UTC). Radio Science detected a signal a few moments later at 17:18:27 UTC at both the ESA Perth antennas and the DSN Canberra DSS-45 and DSS-34 antennas, each with a full spectrum recording as shown in Figure 7. DSS-45 and DSS-34 acquired a closed-loop lock on the signal a few moments later at 17:18:32 UTC.

5. DEEP SPACE MANEUVERS

While en-route to Jupiter, two Deep Space Maneuvers (DSMs) were executed by the Juno spacecraft in order to increase its velocity with respect to the sun. DSM1 was

executed on August 30, 2012, 22:30 UTC and DSM2 was executed on September 4, 2012, 22:30 UTC. Although not time-sensitive maneuvers, MFSK tones were used to determine real-time spacecraft state due to the risk and low signal-to-noise ratios associated with the orientation needed when using the main engine.

Prior to DSM-1, a preparation campaign was conducted to ensure operational readiness for supporting the critical events. The preparation campaign included hardware and software unit testing within the EDA systems, a full simulation of the DSMs in the testbed, an integrated Operational Readiness Test (ORT) with the project, and an in-flight tones test with the end-to-end flight and tones system.

Timeline of Events

Both DSM-1 and DSM-2 followed a similar timeline of events; however, the burns occurred on different days. The maneuver was designed to occur during a period of time where both the Goldstone Deep Space Communications Complex (GDSCC) and Canberra Deep Space Communications Complex (CDSCC) could see the spacecraft.

Table 5. Abbreviated timeline of events for the DSMs. Both DSM-1 and DSM-2 followed the same timeline; but on different days. Times are reception time at Earth.

| Time (UTC) | Event |
|------------|----------------------------------|
| 13:30:00 | GDSCC Beginning of Track |
| 20:50:00 | CDSCC Beginning of Track |
| 21:07:27 | Start of Tones |
| 21:07:47 | Swap from HGA to MGA |
| 21:13:25 | Precession to 15 deg off-Point |
| 21:29:47 | Precession Completed |
| 22:13:50 | Start Precession to DSM Attitude |
| 22:27:15 | Swap from MGA to TLGA |
| 22:31:05 | Precession Completed |
| 22:42:05 | Spin-up from 2 RPM to 5 RPM |
| 22:47:03 | Spin-up Completed |
| 22:57:05 | Start Main Engine Burn |
| 23:26:58 | End Main Engine Burn |
| 23:29:07 | Spin-down from 5 RPM to 2 RPM |
| 23:33:51 | Spin-down Completed |
| 23:40:40 | Start Precession to Sun-point |
| 23:44:38 | Swap from TLGA to MGA |
| 23:50:10 | End of Tones |
| 00:00:45 | Precession Completed |
| 01:05:00 | GDSCC End of Track |
| 06:10:00 | CDSCC End of Track |

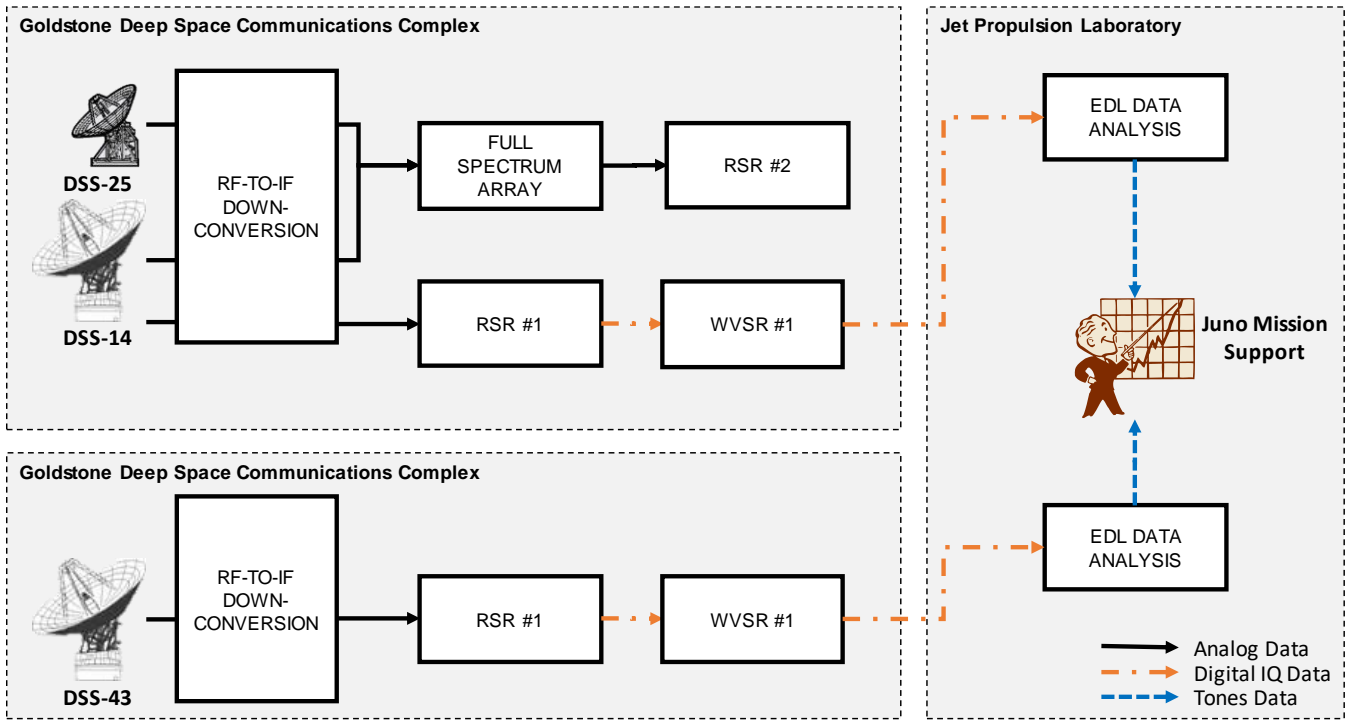


Figure 8. DSN configuration and data flow for the Deep Space Maneuvers. The 70-m DSS-14 antennas were the primary tones data flow. In addition, the Full Spectrum Processor Array (FSPA) was used to array DSS-14 and DSS-25 together for post-processing and testing only (no real-time data flow).

Just before the maneuver, the spacecraft telecommunications system reconfigured to transmit tones instead of telemetry (Table 5). The spacecraft then swapped to the MGA and performed an initial turn 15 degrees off-Earth point in the direction of the maneuver attitude (Juno is a spin-stabilized spacecraft; turns are performed via *precessions* to change the direction of the spin-axis rather than a direct turn). The spacecraft maintained this attitude for nearly an hour to perform configuration of the propulsion system and stabilize the attitude via nutation dampening. The spacecraft then turned to nearly 90 degrees off-Earth point to perform the maneuver. During this turn, the spacecraft swapped to the TLGA. At this attitude, the spacecraft spun up from the nominal spin rate of 2 RPM to 5 RPM for better stabilization when the main engine fired. When the spacecraft completed the maneuver, it spun back down to the nominal 2 RPM and initialized a turn back to Sun-point to recharge the solar panels. During the turn, the spacecraft swapped back from the TLGA to the MGA, disabled tones, and began transmitting a low-rate telemetry at 100 bits per second.

DSN Configuration

DSM-1 and DSM-2 were nearly identical in DSN configuration, which is shown in Figure 8. The 70-meter DSS-14 (Goldstone) and 70-meter DSS-43 (Canberra) antennas supported simultaneously. At Goldstone, a single 34-meter antenna, DSS-25, was arrayed with DSS-14 as a test case – tones had never before been utilized with an array, and this would serve as a test for the JOI maneuver later in the mission. The arraying was performed by the Full Spectrum Processor Array (FSPA) assembly.

Each antenna’s signal was recorded by the Radio Science Receiver (RSR). The digital IQ data were then piped through the brand-new (at the time) Wideband VLBI Science Receiver (WVSR) because the WVSR had a higher network throughput for real-time transmission back to JPL. The EDAs received the digital IQ data and performed tones decoding. The tones data were then shown to the project in the mission support areas (at JPL and Lockheed Martin).

Results and Performance

During DSM-1, tone data was recovered above 90% in real-time and 100% during post-processing (Table 6). Correct tone detection is computed based on the telemetry recorded

Table 6. Correct tone detection percentage from DSM-1.

| DSN Configuration | Real-time | Post-Processing |
|-------------------|-----------|-----------------|
| DSS-14 | 91.7% | 100% |
| DSS-43 | 95.3% | 100% |

Table 7. Correct tone detection percentage from DSM-2.

| DSN Configuration | Real-time | Post-Processing |
|-------------------|-----------|-----------------|
| DSS-14 | 83.2% * | 83.2% * |
| DSS-25 | N/A | 94.2% |
| DSS-43 | 99.8% | 100% |

* A maintenance related failure caused a 13-minute outage. Tones were interrupted during this time

on-board the spacecraft of which tones were commanded by the flight software and is defined as *total seconds* of correct tones divided by the total duration of tones. Tones often last longer than their minimum time of 3 seconds. The error rate accounts for both false detection and missed tones. The 91.7% and 95.3% performance in real-time corresponds with 3 tone events missed; this was primarily due to a configuration issue, where the EDAs halted processing early. During post-processing, the EDA is reconfigured to process tones data to compensate for precise frequency dynamics, and 100% of tones were recovered. Post-processing with this level of precision took ~8 hours in this case.

The configuration error was fixed for DSM-2, resulting in 99.8% real-time correct tone detection from DSS-43. At DSS-14, a maintenance-related failure caused a 13-minute outage in data flow which could not be recovered during post-processing.

The FSPA assembly did not perform as expected for either DSM-1 or DSM-2: the signal-to-noise ratio must be accurately modeled for precise arraying, and variations in signal-to-noise ratio were not modeled by the system, which was not designed for this type of event. On DSM-2, tones were also recorded only by DSS-25 and post-processed to provide an additional performance metric: 94.2% of tones were recovered. This is fairly close to a model prediction (Figure 6), since the signal-to-noise ratio at DSS-25 is 6 dB-Hz lower than DSS-14.

6. EARTH FLYBY

On October 9, 2013, Juno conducted a gravitational assist flyby of Earth. This was a necessary flyby to increase the spacecraft's velocity relative to the Sun in order to reach Jupiter. During the Earth flyby, Juno would enter an eclipse and go into Earth's shadow for the first time.

A Radio Science investigation was proposed to investigate anomalous spacecraft velocity changes that have been observed prior to Juno [13]. This would require coherent 2-way Doppler for 4 days around Earth closest approach, including the use of the European Space Agency's Malargüe and Perth Deep Space Antennas (the ESTRACK network) to reduce the coverage gap at closest approach from 3.5 hours to only 29 minutes. The Radio Science team supported the flyby in real-time to monitor the X-band signal from Juno at both the DSN and ESTRACK networks. A safe mode entry would be detected with a ~4-minute outage of X-band as the TWTA is power cycled and warms up, followed by the presence of a carrier with a telemetry-encoded subcarrier at 25 kHz.

The spacecraft entered eclipse at 19:19 UTC and flew by closest approach at 19:21 UTC. Ten minutes later, at 19:31 UTC, the spacecraft entered safe mode. Due to the flyby geometry, there was a gap in coverage around closest approach and the safe mode entry was not detected immediately. Upon the spacecraft rising above the Madrid complex, it was evident that the spacecraft was in safe mode

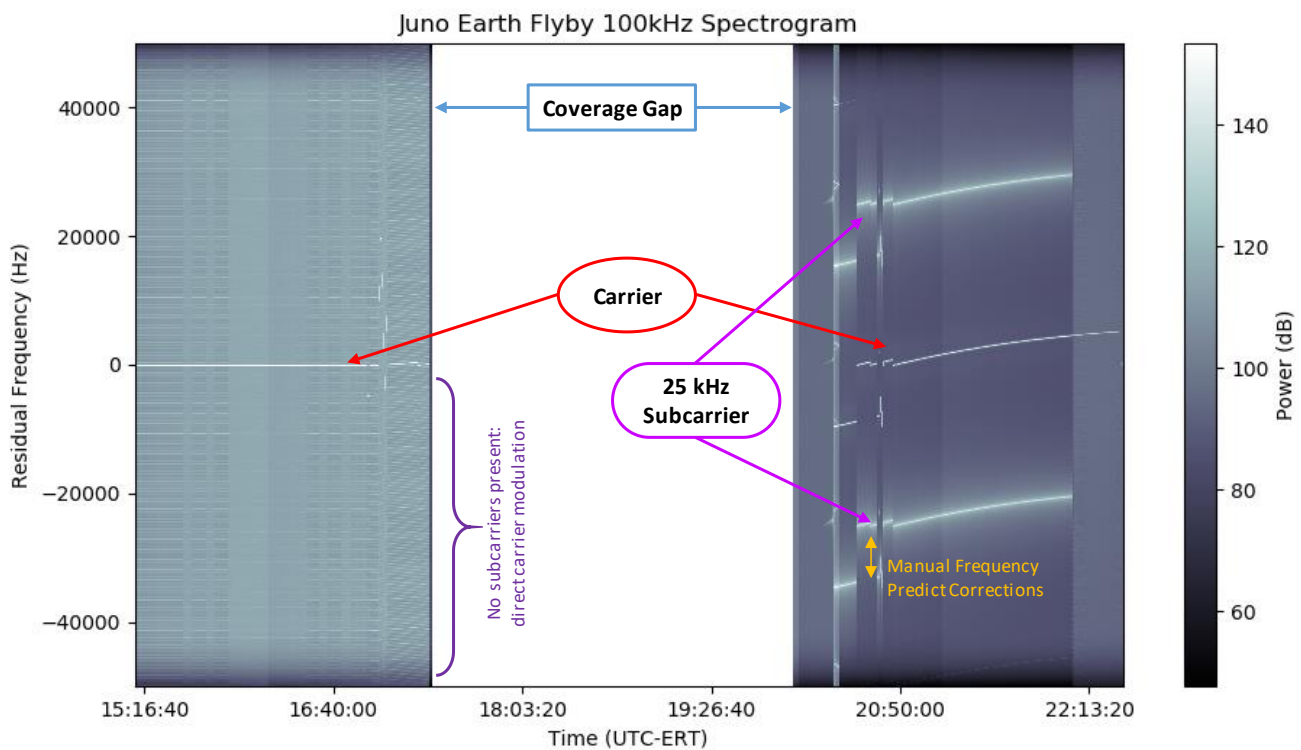


Figure 9. Juno's full spectrum during Earth Flyby. Both the first of the data, ending at ~17:20 UTC, and second part, beginning at ~20:00 UTC, are from the Madrid DSN complex. Annotated are the primary differences in the spectra: the 25 kHz telemetry-encoded subcarrier is indicative of a safe mode entry (no telecom reconfiguration was nominally planned during this time).

through the spectrum, as 25 kHz subcarriers were present as shown in Figure 9.

The safe mode was later traced to the battery voltage falling below the threshold value [15]. Additionally, no anomalous spacecraft velocity changes were detected [14].

7. JUPITER ORBIT INSERTION (JOI)

The Jupiter Orbit Insertion (JOI) was a main engine maneuver executed on July 5, 2016, 02:30 UTC. The maneuver was designed to slow the Juno spacecraft down upon its arrival at Jupiter in order to enter orbit. This was not only a time-critical event, but a high-risk event as this would be the first time Juno experienced the high radiation and dynamical environment of Jupiter. MSFK tones were prime for communication during the main engine maneuver because the signal-to-noise ratio and doppler dynamics were too large for real-time telemetry. A second maneuver, to be performed in October 2016, was planned to reduce the orbital period from 53 days to 14 days, but was cancelled.

Due to the real-time criticality of the event, a major preparation campaign, both within the radio science team and the project as whole, was taken on to ensure readiness for the maneuver. Lessons learned from the DSM-1 and DSM-2 events were incorporated into an update into the EDA configuration and displays. Lab simulations were performed using the expected signal power levels and frequency dynamics with the EDA hardware. A full end-to-end system test was performed in November 2015 with the spacecraft transmitting tones for reception in the same DSN configuration that was to be used during the JOI maneuver.

Additionally, during the time between the DSMs and JOI, the FSPA assembly was replaced with the DSCC Downlink Array (DDA) assembly for antenna arraying. After the end-to-end test in November 2015, software updates were made to the DDA to improve performance of the arraying assembly with tones. Another end-to-end test was performed in March 2016 to validate the DDA performance with these upgrades. DSN readiness tests using the same JOI configuration were performed in June 2016 with the spacecraft transmitting carrier-only (no tones).

Timeline of Events

The timeline and series of events for JOI (Table 8) is nearly identical to that of the DSMs. The primary differences between the DSMs and JOI are the duration of each event, attitudes, and onboard fault protection configuration. From the perspective of the communications, the ground configuration was more complex due to the large number of antennas utilized (total of nine antennas).

Tones started during the Goldstone coverage, mid-way through the track. After tones began, the spacecraft swapped from the HGA to the MGA while conducting a turn 15 degrees toward the maneuver attitude. The spacecraft remained there for a little over one hour while the propulsion

Table 8. Abbreviated timeline events for JOI, which contain the same set of events as the DSMs, but at different attitudes and times. The local time begins on July 4, 2016, and crosses midnight of July 5, 2016.

| Time (UTC) | Time (PJ) | Event |
|------------|-----------|----------------------------------|
| 18:25:00 | -09:10 | GDSCC Beginning of Track |
| 01:13:47 | -02:22 | Start of Tones |
| 01:14:13 | -02:21 | Swap from HGA to MGA |
| 01:16:47 | -02:19 | Precession to 15 deg off-Point |
| 01:32:16 | -02:03 | Precession Completed |
| 01:40:00 | -01:55 | CDSCC Beginning of Track |
| 02:28:13 | -01:07 | Start Precession to JOI Attitude |
| 02:41:41 | -00:54 | Swap from MGA to TLGA |
| 02:53:06 | -00:42 | Precession Completed |
| 02:56:28 | -00:39 | Spin-up from 2 RPM to 5 RPM |
| 03:01:26 | -00:34 | Spin-up Completed |
| 03:18:25 | -00:17 | Start Main Engine Burn |
| 03:35:53 | 00:00 | Jupiter Closest Approach |
| 03:53:22 | +00:17 | End Main Engine Burn |
| 03:55:35 | +00:19 | Spin-down from 5 RPM to 2 RPM |
| 04:00:19 | +00:24 | Spin-down Completed |
| 04:07:11 | +00:31 | Start Precession to Sun-point |
| 04:11:12 | +00:35 | Swap from TLGA to MGA |
| 04:16:39 | +00:40 | End of Tones |
| 04:27:16 | +00:51 | Precession Completed |
| 05:50:00 | +02:14 | GDSCC End of Track |
| 11:30:00 | +07:54 | CDSCC End of Track |

system was configured and attitude stabilized. Canberra antennas began tracking during this time period. The spacecraft then performed a fast turn to the maneuver attitude while swapping antennas from the MGA to the TLGA. After arriving at the maneuver attitude, the spacecraft increased its spin rate from 2 RPM to 5 RPM to improve pointing performance during the main engine firing. The main engine firing is centered around closest approach (perijove). There is both an Inertial Measurement Unit (IMU) to measure the velocity change and a timer cutoff for maximum burn duration. After the main engine burn was completed, the spacecraft spun back down to 2 RPM and began to turn to Sun-point to recharge the solar panels. During the turn, the spacecraft swapped back to the MGA, disabled tones, and began transmitting telemetry at 100 bits per second. At each antenna swap, a momentary loss of signal occurred while the telecom system reconfigured for that antenna.

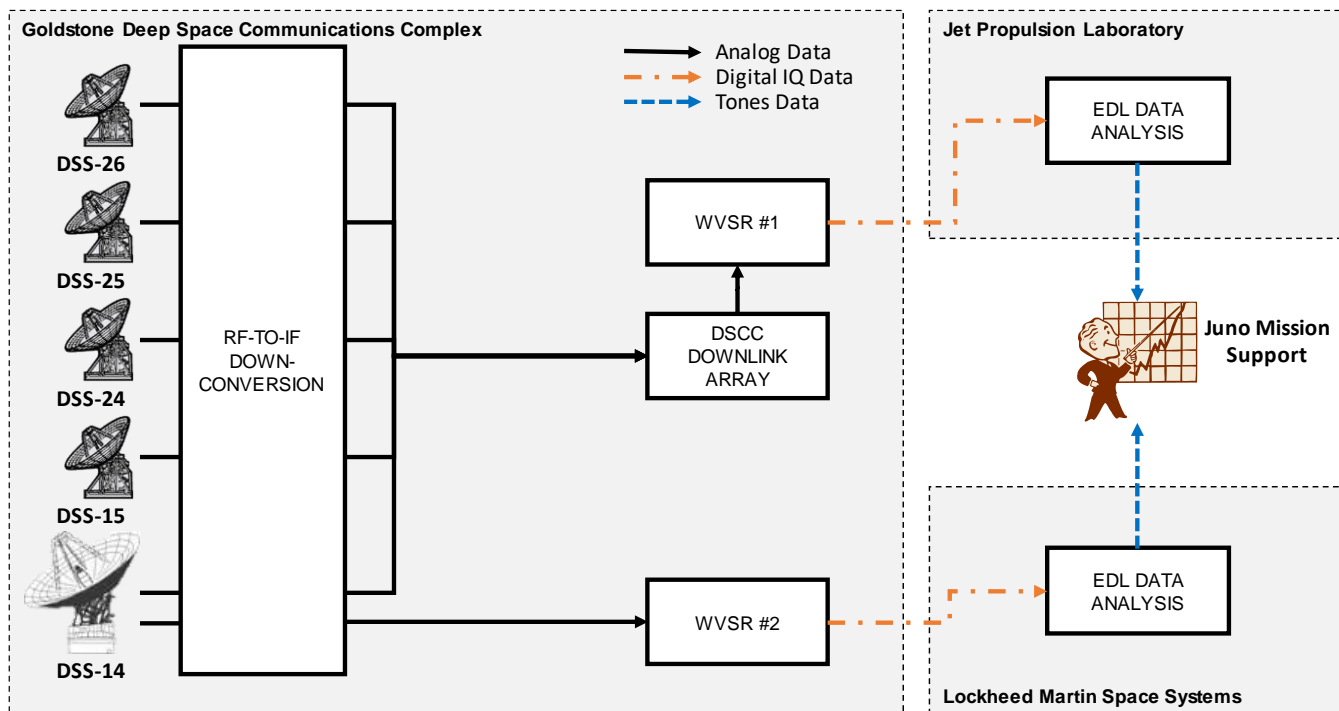


Figure 10. DSN configuration and data flow for Jupiter Orbit Insertion from the Goldstone Deep Space Communications Complex. Data from each 34-m station (DSS-15, -24, -25, -26) plus the 70-m station (DSS-14) was fed into an array to improve the signal strength for tones decoding at an EDA. Additionally, data from the 70-m DSS-14 station was fed directly into an EDA in the event of an anomaly in the array. Configuration for the Canberra Deep Space Communications Complex was identical, but with one less 34-m station.

DSN Configuration

JOI was covered by both Goldstone and Canberra. At Goldstone, five antennas were used: 70-meter DSS-14 and 34-meter DSS-15, DSS-24, DSS-25, and DSS-26. All antennas were arrayed together for an extra ~2.6 dB of signal gain above the level of the 70-meter. This provided enough signal gain to meet the 99% tone detection requirement. At Canberra, all four antennas were used: 70-meter DSS-43 and 34-meter DSS-45, DSS-34, and DSS-35. Figure 10 shows the DSN configuration for Goldstone only. The Canberra configuration was identical, but with one less 34-meter antenna.

Unlike DSMs, the RSR was not used as the primary data recorder and piped into the EDAs. The WVSRs had matured to the point where they could be relied on for the primary data recording and digital data source. The RSRs were used as a backup recording, with one RSR recording each individual antenna. The WVSRs recorded and piped the digital IQ data from the DDA assembly and 70-meter antennas to the EDA systems, which were split between JPL (Pasadena, CA) and Lockheed Martin Space Systems (Littleton, CO). Four EDAs ran simultaneously: one receiving data from the Goldstone array, one receiving data from DSS-14, one receiving data from the Canberra array, and one receiving data from DSS-43. Tones data were displayed at both mission support areas simultaneously.

Tones Results and Performance

The first tone was detected at Goldstone at 01:13:47 UTC and the last tone ended at 04:05:51 UTC, during the turn to Sun-pointing after the maneuver. Canberra began detecting tones at the beginning of track at 01:35:00 UTC.

Correct tone detection (total duration of correct tones divided by total duration of tones) at Canberra was 99.9% on DSS-43 only and 100% on the array. At Goldstone, only 93.7% of tones were correctly detected. This was due to a software configuration issue with the EDA, where the size of the processed recordings being streamed to the EDAs exceeded their maximum data buffer size. The Goldstone recording started earlier than the Canberra recordings, so this was not an issue at Canberra. All tones were recovered during post-processing for Goldstone.

Table 9. Correct tone detection percentage from JOI.

| DSN Configuration | Real-time | Post-Processing |
|-------------------|-----------|-----------------|
| GDSCC Array | 93.7% | 100% |
| DSS-14 Only | 93.7% | 99.9% |
| CDSCC Array | 100% | 100% |
| DSS-43 Only | 99.9% | 99.9% |

2016/186 JOI Goldstone Array Pc/No

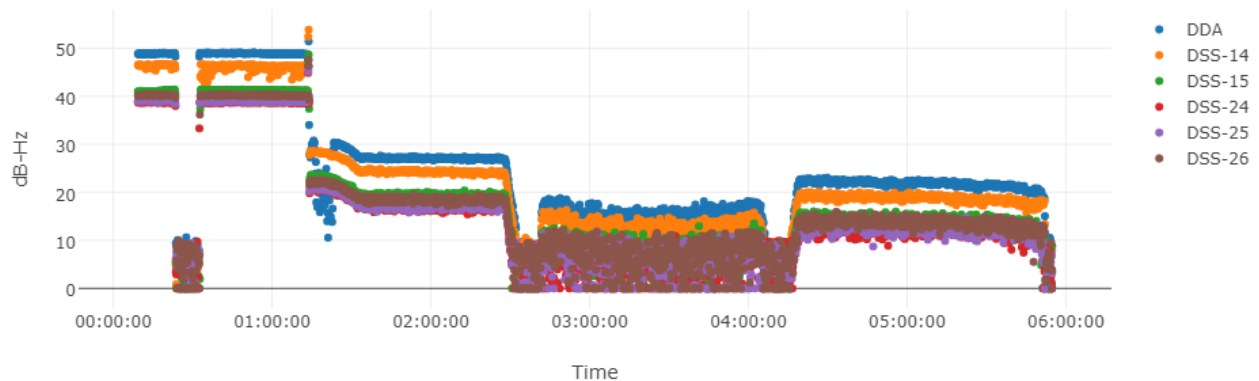


Figure 11. Carrier Signal-to-Noise Ratio during Jupiter Orbit Insertion from antennas at the Goldstone Deep Space Communications Complex. The DSCC Downlink Array (DDA) assembly combined power from each antenna for a ~2.6 dB-Hz gain over DSS-14 alone.

The issue was not discovered during the readiness tests prior to JOI because the tests did not stream data from the WVSR to the EDA for as long of a duration. An additional challenge was that the final JOI Operational Readiness Test (where this issue would have been detected) was cancelled due to investigation of a possible related flight issue. After JOI, the EDA maximum buffer size was updated in its configuration file to support these longer recordings and documentation was updated accordingly.

At the 70-meter antennas, 6-8 seconds of tone false detections were seen, giving 99.9% correct detection. During this duration, the signal-to-noise ratio was below the threshold and was flagged as “low” in real-time, indicating a potential false detection. This was true in both real-time and post-processing.

Array Results and Performance

At Goldstone, the DDA assembly provided an arraying capability to combine power from DSS-14, DSS-15, DSS-24, DSS-25, and DSS-26. The DDA was also used at the Canberra complex.

The carrier signal-to-noise ratios from Goldstone are presented in Figure 11 as an example. During JOI, the array slightly exceeded expectations. The array measured an average carrier signal-to-noise ratio during the time on the TLGA (the most critical portion) of 14.4 dB-Hz compared with 12.9 dB-Hz at DSS-14 alone, providing a signal gain of ~2.5 dB-Hz. The Canberra array performed within expectations as well, with a performance gain of ~1.9 dB-Hz over the nominal level at DSS-43 (the gain was not as high as

Goldstone because Canberra had one less 34-meter antenna in the array).

Doppler Event Detection

In addition to detecting events via tones, any dynamical effect which induces a velocity change relative to the phase center of the antenna will have an impact on the signal’s Doppler shift as received at Earth. Major dynamical effect changes during JOI include the turns to/from maneuver attitude, the maneuver itself, changes in the spacecraft spin rate, and antenna changes.

Figure 12 shows a plot of the residual frequency around the main engine burn. In this plot, dynamical effects from the spacecraft trajectory and main engine burn are included in the predicted frequency. The remaining residual frequency is dominated by uncertainties in the main engine performance, the spacecraft spin signature, and instability of the spacecraft’s onboard oscillator (frequency reference). Key events that are detectable in the Doppler shift are highlighted on the plot. At 02:34, the spacecraft turned to the optimal burn direction and switched to utilizing the TLGA antenna. In the residual frequency, the amplitude of oscillation increases due to the antenna switch because the antenna is located at a different location relative to the spin axis. At 02:56, the spacecraft increased its spin rate from 2 RPM to 5 RPM. The residual frequency periodicity increases in frequency and amplitude corresponding to this spin rate increase. The main engine burn itself is not clearly seen because the modeled frequency was quite close to the actual Doppler shift. At 03:55, the spacecraft reduced its spin rate from 5 RPM back to 2 RPM, and at 04:06 the spacecraft changed to a sun-point attitude to recharge the batteries and

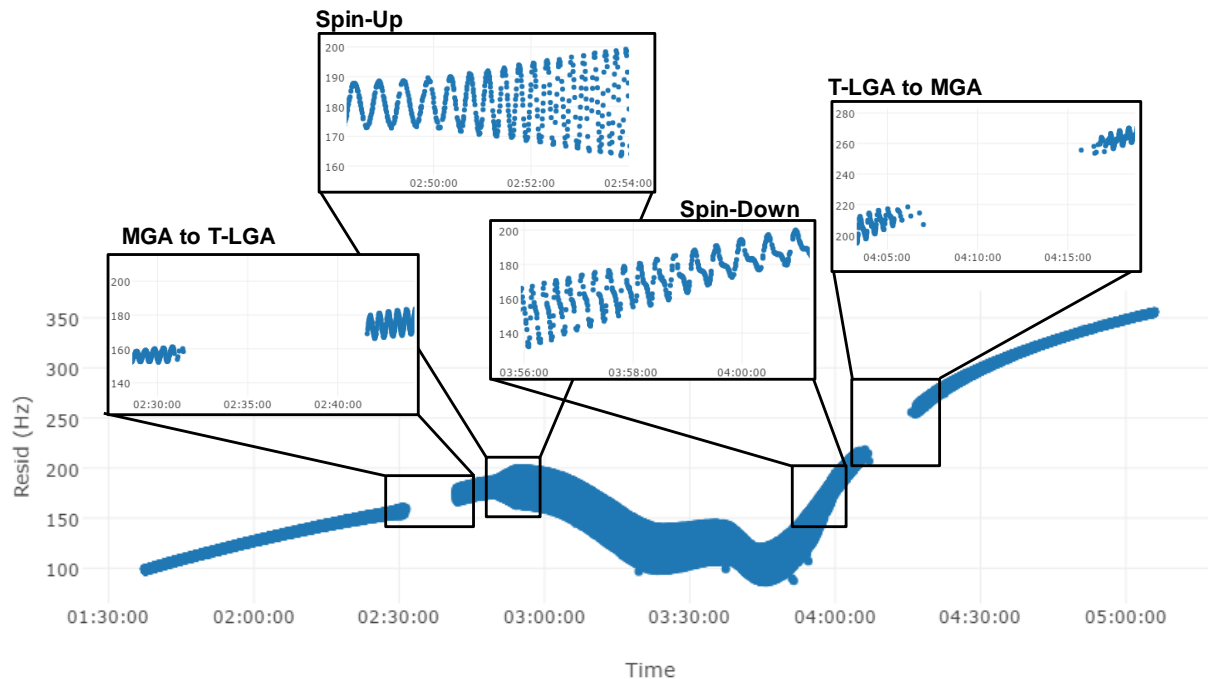


Figure 12. Frequency residuals observed during JOI by the Radio Science Receiver. The predicted accounts for the predicted trajectory and the main engine burn, but not the spin signatures due to spacecraft rotation.

returned to the MGA. The corresponding changes in frequency were observed as noted in the figure.

It is possible to detect more events with the Doppler shift than those presented here. The predicted frequency used in this analysis already accounts for the main engine firing. If that is not included in the modeled frequency, a sharp cutoff would be seen in the Doppler shift as the main engine changes the velocity of the spacecraft. Another sharp cutoff would be seen after main engine cutoff. This technique was performed during Cassini’s Saturn Orbit Insertion in 2004 [16] and is similar to how parachute deployment detection was done with Mars EDL on Curiosity [6] and InSight. This technique was applied by the Juno Navigation team to verify that the main engine firing was executing within expectations. Tones provide more information regarding specific events that cannot be reconstructed through Doppler shift analysis alone.

In the event of a partial or failed maneuver, the predicted frequency would no longer be accurate. In the case of Juno’s JOI, the residual frequency would slowly begin to drift off. Although this frequency error grows very large over time, the frequency rate and frequency accelerations are small in comparison to the spin signature dynamics, approximately 0.3 Hz/sec.

8. PERIJOVES

Juno entered into a 53-day orbit around Jupiter during JOI. Although a second maneuver, called the Period Reduction Maneuver (PRM) was planned to occur two orbits after JOI in October 2019, the maneuver was not executed due to an

issue discovered with the propulsion system. During the PRM, the spacecraft would have been executing a main engine maneuver similar to that done during JOI, including utilization of MSFK tones to determine the state of the spacecraft.

Although the Juno spacecraft is capable of many attitudes to accomplish the science objectives [17], they can be grouped into two different types of perijoves: a Gravity Science perijove and an Off-Axis Attitude perijove. During a Gravity Science perijove, the spacecraft is on Earth-point to use the High-Gain Antenna. During an Off-Axis Attitude perijove, the spacecraft is not on Earth-point and uses the MGA or FLGA for communications.

During any perijove segment, the spacecraft flies by the planet through the radiation belts inbound to the planet, dives beneath the radiation, then goes through the radiation belts again on the outbound. During Juno’s lifetime, it will experience a total ionizing dose of 20.5 krad [17]. Perijoves are critical activities for the Juno mission due to the science collected during perijove balanced with the risks associated with flying through the intense radiation and extreme acceleration dynamics.

Gravity Science Perijoves

During a Gravity Science perijove, the High Gain Antenna is pointed directly to Earth for communications at X-band and Ka-band. Due to the high signal-to-noise ratio during a Gravity Science perijove, there is an active telemetry stream from the spacecraft which provides the spacecraft’s health

and safety directly. Any anomalous signal levels or frequencies will be detected in the full-spectrum open-loop recorders. If a system fault monitor detects an error on the spacecraft, it may enter safe mode. During a safe mode entry, the Ka-band signal will be disabled alongside a ~4-minute outage of X-band as the TWTA is power cycled. Afterwards, safe mode will swap to the MGA with telemetry encoded on 25-kHz subcarriers. This signal configuration is easily detectable within the open-loop receivers, and was demonstrated during the Earth flyby.

Off-Axis Attitude Perijoves

During an Off-Axis Attitude (OAA) perijove, the spacecraft points the remote sensing instruments either to nadir (called an “MWR” attitude, for the MicroWave Radiometer to point to the surface) or close-to nadir (called an “Off-Axis Attitude”, a general term).

During an OAA perijove, the Juno spacecraft is off Earth-point by up to ~35 degrees and utilizes the MGA or FLGA for communications at X-band only. The signal levels during a typical OAA pass are low, ~7-12 dB-Hz, and often cannot be detected with the closed-loop receiver at the DSN. However, the open-loop receivers can detect this signal clearly.

During a nominal OAA perijove, the signal is carrier only (no telemetry encoding), so the spacecraft’s state must be observed through the carrier only. The observables for a nominal spacecraft state are:

- Carrier-only at the expected signal-to-noise ratio
- Nominal spin signature on the Doppler shift

If a safe mode entry is observed in real-time, the same response as during a Gravity Science perijove is seen. Afterwards, an off-nominal spacecraft state is observed with:

- Detection of subcarrier with telemetry encoding
- Change in signal-to-noise ratio, corresponding with the spacecraft turning to gain energy on the solar panels
- Lack of spin signature or different spin signature

Thus far, all OAA attitudes have been successful, and only the nominal spacecraft state has been detected during these perijoves.

9. CONCLUSION

Juno Radio Science has provided crucial support to the Juno mission in both a science and engineering capacity to ensure a successful mission. Radio Science engineering support allowed for confirmation of successful mission milestones: launch, main engine maneuvers, Earth gravity assist flyby, and Jupiter perijoves with high signal dynamics and low signal-to-noise ratio.

Open-loop recordings have flexibility that allow for unique applications. As demonstrated with the EDA system during

the DSM and JOI maneuvers, real-time streaming and data processing provided crucial insight into the state of the spacecraft. Tones were planned for use on a period reduction maneuver (PRM), but the maneuver was cancelled after a risk was identified in the propulsion system.

Lessons learned from Juno critical event support should be applied to future missions:

1. *Account for frequency accelerations.* Juno saw large, unpredictable frequency dynamics coming from the spin signature of an off-axis antenna. The spin phase of the spacecraft cannot be predicted on the ground well-enough to account for it in the Doppler frequency predicts. The theoretical model for configuration of the EDA did not account for non-zero frequency accelerations. In lieu of developing new models, simulated data was generated and processed to determine probability of detection of tones and the DDA was utilized to help account for these frequency dynamics. Future missions should improve on the theory to account for non-zero frequency accelerations or perform robust simulations to validate the system performance.
2. *Incorporate tones into the telecom testbed.* A local testbed was not set up for Juno to perform a full-system validation. MSL utilized a testbed at JPL [7], which helped validate the performance of tones and the EDA, in addition to the in-flight tones tests performed by both MSL and Juno. In the absence of a Juno telecom testbed at JPL, simulations were performed as described in Section 3.
3. *Verify system operations with a full system-level test on the same timeline prior to the event.* Although several in-flight tests were performed, the final Operational Readiness Test for JOI was cancelled. The final Operational Readiness Test would have been on the same timeline as the event itself. This would have helped uncover the EDA maximum record size issue, which caused an ~11-minute outage of tones during JOI. Future missions should plan on running through the full timeline and configuration prior to the event.
4. *Simultaneous processing from multiple downlink paths.* Having multiple downlink paths reduces the risk of a station- or EDA-related failure causing outage of data. During DSM-2, a DSN maintenance-related failure caused an outage in tones data from Goldstone; however, the data were recovered from the Canberra downlink path. During JOI, the Goldstone EDAs stopped processing due to a buffer size issue; however, the data were recovered fully in post-processing and in real-time from the Canberra downlink paths. Future missions should continue to utilize multiple antennas and downlink paths for communications support.

In the foreseeable future, with a healthy Juno spacecraft, the Juno radio science team will continue monitoring critical events with the radio science open-loop receivers for diagnostic and logistical support. An integrated and supported radio science team in a mission system provides crucial and high-quality support for not only a science investigation, but for critical events as well. The Europa Clipper mission, which will launch in 2023 and will explore Jupiter's moon, Europa, plans to use MFSK tones for communications during JOI. Other future missions can also leverage from the communications techniques described in this paper.

ACKNOWLEDGEMENTS

This work was carried out at the Jet Propulsion Laboratory, California Institute of Technology, under a contract with the National Aeronautics and Space Administration. The authors would like to thank Ed Hirst, Matt Johnson, and John Bordi for their leadership in mission management, Juno telecommunications engineers Mark Susak and Chris Leeds at Lockheed Martin, and the rest of the Juno mission operations team.

© 2019 California Institute of Technology. Government sponsorship acknowledged.

REFERENCES

- [1] Bolton, S.J., et al. (2017), *The Juno Mission*, Space Science Reviews, 213, 5-37, doi:10.1007/s11214-017-0429-6.
- [2] S.W. Asmar and N.A. Renzetti, *The Deep Space Network as an Instrument for Radio Science Research*. JPL Publication 80-93, Rev. 1 (1993).
- [3] Asmar, S.W., et al. (2017), *The Juno Gravity Science Instrument*, Space Science Reviews, 213, 205-218, doi:10.1007/s11214-017-0428-7.
- [4] Buccino, Dustin, Kahan, Daniel, Yang, Oscar, and Oudrhiri, Kamal, *Initial Operations Experience and Results from the Juno Gravity Experiment*, 2018 IEEE Aerospace Conference, Big Sky, MT, 2018, pp. 1-8.
- [5] Soriano et al, *Spacecraft-to-Earth Communications for Juno and Mars Science Laboratory Critical Events*, 2012 IEEE Aerospace Conference, Big Sky, MT, 2012.
- [6] Oudrhiri, Kamal, et. al. *Sleuthing The MSL EDL Performance From An X Band Carrier Perspective*. 2013 IEEE Aerospace Conference, Big Sky, MT, 2013.
- [7] Soriano et al, *Direct-to-Earth Communications with Mars Science Laboratory during Entry, Descent, and Landing*, 2013 IEEE Aerospace Conference, Big Sky, MT 2013.
- [8] Mukai, Ryan, Hansen, David, Mittskus, Anthony, Taylor, Jim, and Monika Danos. *Juno Telecommunications*. Vol. 16. Pasadena: Jet Propulsion Laboratory, 2012. DESCANSO Design and Performance Summary Series.
- [9] J.D. Vacchione, R.C. Kruid, A. Prata, L.R. Amaro, A.P. Mittskus, *Telecommunications antennas for the Juno Mission to Jupiter*, 2012 IEEE Aerospace Conference, Big Sky, MT, 2012.
- [10] *DSN Telecommunications Link Design Handbook*, DSN No. 810-005, Rev. F, Jet Propulsion Laboratory, Pasadena, CA. <http://deepspace.jpl.nasa.gov/dsndocs/810-005/>
- [11] E. Satorius, P. Estabrook, J. Wilson, D. Fort. *Direct-to-Earth communications and signal processing for Mars exploration rover entry, descent and landing*, The Interplanetary Network Progress Report, IPN Progress Report 42-153, May 2003.
- [12] Dutta, Schweta and Soriano, Melissa. *Optimizing Multiple-Frequency Shift Keying during Spacecraft Critical Events for Future Missions*, 2019 IEEE Aerospace Conference, Big Sky, MT, 2019, pp. 1-10.
- [13] Anderson, J.D., J.K. Campbell, J.E. Ekelund, J. Ellis, and J.F. Jordan, *Anomalous Orbital-Energy Changes Observed during Spacecraft Flybys of Earth*, Phys. Rev. Lett., 100, 2008
- [14] Thompson, Paul F., Abrahamson, M., Ardalan, S., and Bordi, J. *Reconstruction of Earth Flyby by the Juno Spacecraft*, 24th AAS/AIAA Space Flight Mechanics Meeting, Jan 14-30, 2014, pp. 1-14.
- [15] Stephens, Stuart, *The Juno mission to Jupiter: Lessons from cruise and plans for orbital operations and science return*, 2015 IEEE Aerospace Conference, Big Sky, MT, 2015, pp. 1-20.
- [16] Asmar, S.W., D.V Johnson, E. Maize, and R.T. Mitchell, *Critical Monitoring of the Cassini Saturn Orbit Insertion Maneuver*, AIAA SpaceOps Conference, Montreal, Canada, May 17-21, 2004.
- [17] Stephens, Stuart. *Juno at Jupiter: The Mission and Its Path to Unveiling Secrets of the History of the Solar System*, 2018 IEEE Aerospace Conference, Big Sky, MT, 2018, pp. 1-19.

BIOGRAPHY



Dustin Buccino is a member of the Planetary Radar and Radio Science Group at NASA's Jet Propulsion Lab. Since joining the group in 2013, he has provided scientific and engineering support to the Cassini, Dawn, InSight, GRAIL, and Juno missions. His research interests include gravity

science, navigation, and tracking of spacecraft. Buccino is currently the instrument operations lead for the Juno Gravity Science investigation.



Melissa Soriano is a senior communications systems engineer in the Communications, Tracking, and Radar Division at the Jet Propulsion Laboratory. Melissa is part of the flight system engineering team for Europa Clipper. She has developed real-time software for Direct-To-Earth communications with Mars Science Laboratory during

Entry, Descent, and Landing, the Long Wavelength Array, NASA's Breadboard Array, and the Wideband VLBI Science Receiver used in the Deep Space Network. Melissa is also currently the software cognizant engineer for the DSCC Downlink Array. She has a B.S. from Caltech, double major in Electrical and Computer Engineering and Business Economics and Management. She also has an M.S. in Computer Science from George Mason University.



Andre Jongeling joined JPL in 1991 where he is currently the Deputy Manager of the Communications Ground Systems Section and the System Engineer for the Common Platform development project. Previously he has been both an engineer and supervisor for JPL's Processor Systems Development Group. Andre

has been involved in the development of a number of advanced systems for use in the DSN in the fields of Radio Science, Radio Astronomy, VLBI, and Antenna Arraying.



Sue Finley has been an employee of NASA's Jet Propulsion Laboratory (JPL) since January 1958, making her the longest-serving woman in NASA. Two days before Explorer 1 was launched, Finley began her career with the laboratory as a human computer, calculating rocket launch trajectories by hand. She now serves as a subsystem engineer for NASA's Deep

Space Network (DSN). At JPL, she has participated in the exploration of the Moon, the Sun, all the planets, and other bodies in the Solar System.



Oscar Yang is a Signal Analysis Engineer in the Planetary Radar and Radio Science Group at the Jet Propulsion Laboratory (JPL). He received his Ph.D. from the Aeronautics and Astronautics Engineering Department at Purdue University. His current research focuses on remote sensing of earth and planetary atmospheric and ionospheric disturbances using radio

science and airglow measurements.



Daniel Kahan is a senior member of the Planetary Radar and Radio Science Group at NASA's Jet Propulsion Laboratory. He has provided engineering support for the radio science community on multiple NASA missions including Mars Global Surveyor, Mars Reconnaissance Orbiter, the GRAIL lunar mission, the International Cassini mission to Saturn, Mars Science Laboratory, InSight, and Juno.



Kamal Oudrhiri is the manager of the Planetary Radar and Radio Science Group at NASA's Jet Propulsion Laboratory and is currently the project manager of the Cold Atom Laboratory. Oudrhiri has led multi-disciplinary teams through the design, implementation and delivery of flight hardware to the radio science community. Over the last decade, Oudrhiri

served in key roles on multiple NASA missions.